UC Davis
UC Davis Previously Published Works

Title

NK Cells Preferentially Target Tumor Cells with a Cancer Stem Cell Phenotype

Permalink

Journal

The Journal of Immunology, 195(8)

ISSN

0022-1767

Authors

Ames, Erik
Canter, Robert J
Grossenbacher, Steven K
et al.

Publication Date

2015-10-15

DOI

10.4049/jimmunol.1500447

Peer reviewed

NK Cells Preferentially Target Tumor Cells with a Cancer Stem Cell Phenotype

Erik Ames[*], **Robert J. Canter**[†], **Steven K. Grossenbacher**[*], **Stephanie Mac**[*], **Mingyi Chen**[‡], **Rachel C. Smith**[*], **Takeshi Hagino**[*], **Jessica Perez-Cunningham**[*], **Gail D. Sckisel**[*], **Shiro Urayama**[§], **Arta M. Monjazeb**[¶], **Ruben C. Fragoso**[¶], **Thomas J. Sayers**[||], and **William J. Murphy**[*,#]

[*]Department of Dermatology, University of California Davis School of Medicine, Sacramento, CA 95817

[†]Division of Surgical Oncology, Department of Surgery, University of California Davis School of Medicine, Sacramento, CA 95817

[‡]Department of Pathology and Laboratory Medicine, University of California Davis School of Medicine, Sacramento, CA 95817

[§]Division of Gastroenterology and Hepatology, Department of Internal Medicine, University of California Davis Medical Center, Sacramento, CA 95817

[¶]Department of Radiation Oncology, University of California Davis School of Medicine, Sacramento, CA 95817

[||]Basic Sciences Program, Leidos Biomedical Research, Inc., Frederick National Laboratory, Frederick, MD 21702

[#]Division of Hematology and Oncology, Department of Internal Medicine, University of California Davis Medical Center, Sacramento, CA 95817

Abstract

Increasing evidence supports the hypothesis that cancer stem cells (CSCs) are resistant to antiproliferative therapies, able to repopulate tumor bulk, and seed metastasis. NK cells are able to target stem cells as shown by their ability to reject allogeneic hematopoietic stem cells but not solid tissue grafts. Using multiple preclinical models, including NK coculture (autologous and allogeneic) with multiple human cancer cell lines and dissociated primary cancer specimens and NK transfer in NSG mice harboring orthotopic pancreatic cancer xenografts, we assessed CSC viability, CSC frequency, expression of death receptor ligands, and tumor burden. We demonstrate that activated NK cells are capable of preferentially killing CSCs identified by multiple CSC markers (CD24$^+$/CD44$^+$, CD133$^+$, and aldehyde dehydrogenase^{bright}) from a wide variety of human cancer cell lines in vitro and dissociated primary cancer specimens ex vivo. We observed

Address correspondence and reprint requests to Prof. William J. Murphy, Department of Dermatology, University of California Davis School of Medicine, 2921 Stockton Boulevard, Suite 1630, Sacramento, CA 95817. wmjmurphy@ucdavis.edu.
The online version of this article contains supplemental material.

Disclosures

The authors have no financial conflicts of interest.

comparable effector function of allogeneic and autologous NK cells. We also observed preferential upregulation of NK activation ligands MICA/B, Fas, and DR5 on CSCs. Blocking studies further implicated an NKG2D-dependent mechanism for NK killing of CSCs. Treatment of orthotopic human pancreatic cancer tumor-bearing NSG mice with activated NK cells led to significant reductions in both intratumoral CSCs and tumor burden. Taken together, these data from multiple preclinical models, including a strong reliance on primary human cancer specimens, provide compelling preclinical evidence that activated NK cells preferentially target cancer cells with a CSC phenotype, highlighting the translational potential of NK immunotherapy as part of a combined modality approach for refractory solid malignancies.

Increasing evidence supports the cancer stem cell (CSC) hypothesis, which postulates that a subpopulation of malignant cells is resistant to conventional cytotoxic/antiproliferative therapies (1–3). It is these CSCs that seed tumor relapse and metastasis, even in cases of apparent complete response to systemic therapy. Therefore, therapies that add a specific anti-CSC strategy to standard cytoreductive therapies may translate to more sustained therapeutic effects.

The presence of CSC subpopulations has been identified in nearly all human malignancies, and mounting studies of CSC engraftment in immunocompromised mice and CSC repopulation in long-term in vitro outgrowth assays have validated the CSC phenotype (2, 4, 5). The expression of various surface markers has also been shown to correlate with tumorigenic potential in breast cancer (6–10), pancreatic cancer (11–13), and sarcomas (5, 14–17). In breast cancer, $CD24^{-/low}/CD44^+/$aldehyde dehydrogenase (ALDH)^{bright} cells have been consistently identified as having high tumorigenic potential in both human cell lines and primary tumors (6, 7, 10). Similarly, pancreatic CSCs have been characterized as $CD24^+/CD44^+/$epithelial-specific Ag^+ and ALDH^{bright}, although these markers are not all uniformly assessed in tandem (18). Lastly, although sarcoma CSCs have been less extensively characterized owing to the lower incident rate of this disease, studies have also identified and validated CSC behavior in $CD133^+$ and ALDH^{bright} subpopulations (14, 16, 17).

NK cells represent a subset of cytotoxic lymphocytes that are critical to the innate immune system. NK cells demonstrate an ability to respond to and eradicate tumor cells. Moreover, they are able to recognize cells through direct receptor–ligand interactions (e.g., MICA/B ligands and death receptor 5 of the TNFR superfamily). This allows for rapid NK killing and mitigates the need for ongoing tumor Ag recognition, which is a mechanism of resistance to humorally based antitumor immunotherapies (19). Although adoptive immunotherapy with NK cells has demonstrated success in the treatment of hematologic malignancies, it has been less effective against solid tumors, in large part because of the inability to deliver high enough numbers of activated NK cells (19, 20). However, NK cells have demonstrated the ability to detect and eradicate CSCs as shown by their ability to reject allogeneic hematopoietic stem cells but not solid tissue grafts. CSCs appear to be a preferential target for NK cells through upregulation of stress-induced Ags as well as the ability of NK cells to target nonproliferating cells (21). Therefore, NK-mediated killing is an attractive candidate for targeting of CSCs following the depletion of non-CSCs by antiproliferative therapies.

We hypothesized that CSCs may be sensitive to NK immunotherapy because, unlike traditional cytotoxic therapies, immune cells do not specifically require target cells to be actively dividing to be targeted for lysis. NK cells recognize target cells through a variety of activating and inhibitory receptors. Activating receptors, such as NKG2D and NKG2C, bind MHC-related molecules (such as the polymorphic MHC HLA class I chain–related gene A), which are upregulated during times of cellular stress and/or viral infection. Human NK cell inhibitory receptors are largely composed of the killer cell Ig-like receptor family, the members of which bind HLA class I molecules. NK cells may therefore be uniquely suited to attack CSCs based on reports of low expression of MHC class I on CSCs and possible increased expression of NK recognition ligands (22, 23).

In this study, we show that NK cells preferentially target CSCs compared with non-CSCs in heterogeneous solid tumor populations in multiple preclinical models of pancreatic cancer, breast cancer, and sarcoma, and a clear strength of our data is a reliance on fresh primary tumor specimens for analysis. We show that NK targeting of CSCs is mediated primarily through the interaction of the NKG2D activating receptor with its ligand. Lastly, we demonstrate the NK cell therapy, aimed at targeting CSCs, resulted in superior antitumor efficacy in vivo. Taken together, these results suggest that NK cell–based immunotherapy aimed at targeting CSCs can provide important therapeutic benefit in the combined modality treatment of solid malignancies.

Materials and Methods

Tumor cell lines and primary specimens

Human cancer cell lines (MDA-MB-231, U87MG, A673, BXPC3, U118, and PANC-1) were obtained and authenticated from the American Type Culture Collection (Manassas, VA). Cells were maintained in the American Type Culture Collection recommended culture medium. Primary human tumor resections FSA1, FSA2, FSA3, FSA4, FSA5, FPA1, and FPA2 were obtained immediately after surgery from the University of California Davis Comprehensive Cancer Center Biorepository, which is funded by the National Cancer Institute (NCI P30CA093373). Tumors were dissociated mechanically and treated with collagenase IV at 37°C for 60 min. FPA2 was also expanded for several passages in medium containing epidermal growth factor and basic fibroblast growth factor before use in cytotoxicity assays to expand cell yield. Consent was obtained from all patients before tissue procurement under the auspices of the Institutional Review Board of the University of California Davis.

NK cell isolation

Human NK cells were isolated from leukocyte filters obtained from healthy donors (Delta Blood Bank, Stockton, CA) and cancer patients (University of California Davis Biorepository). Leukocyte filters were back-flushed with PBS and lymphocytes were isolated with lymphocyte separation medium (CellGro, Manassas, VA). Lymphocytes were then resuspended at 5×10^7 cells/ml with 1000 patient-matched RBCs added back per lymphocyte, using a RosetteSep human NK cell enrichment cocktail (StemCell

Technologies, Vancouver, BC, Canada). This protocol typically yielded >95% CD45^{+}/CD56^{+}/CD3^{−} cells.

NK cell activation and expansion

Human NK cells were activated and expanded based on a protocol adapted from Berg et al. (24) The good manufacturing practices–grade EBV-transformed lymphoma cell line EBV-SMI-LCL (provided by Dr. Richard Childs, National Cancer Institute) was used as feeder cells to promote expansion. Isolated NK cells were cultured with 100 Gy gamma-irradiated EBV-SMI-LCL cells at a ratio of 20 lymphoma cells per NK cell in medium containing 500 IU/ml recombinant human (rh) IL-2 (Biological Resources Branch, National Cancer Institute, Frederick, MD). NK cells were grown in X-VIVO 20 (Lonza, Basel, Switzerland) with 10% human male AB serum (Valley Biomedical, Winchester, VA) in upright T-75 flasks each containing no more than 20 ml. Beginning on day 6, cells were adjusted to 6×10^5 cells/ml and allowed to expand 200- to 1000-fold by day 18. Except where noted, we performed all in vitro/ex vivo NK cell experiments using activated rh-IL2, and all NK cells were used between days 12 and 21 after isolation and expansion to ensure optimal activation.

Flow cytometry

Pacific Blue anti-CD45 (HI30), allophycocyanin anti–HLA-ABC (G46-2.6), Alexa Fluor 488 anti-CD3 (UCHT1), and 7-aminoactinomycin D (7-AAD) were purchased from BD Biosciences (San Jose, CA). PE-Cy7 CD24 (ML5), Pacific Blue CD44 (IM7), biotin anti-MICA (6D4), biotin anti-Fas (DX2), and allophycocyanin-Cy7 anti-CD56 (HCD56) were purchased from BioLegend (San Diego, CA). PE anti-CD133 (AC133) was purchased from Miltenyi Biotec (Auburn, CA). PE anti-DR5 (DJR2-4) was purchased from eBioscience (San Diego, CA). We used a linked streptavidin secondary Ab for detection of biotinylated anti-MICA/B and anti-Fas Abs. Live tumor cells were gated and separated from NK cells by discriminating side scatter (SSC)[high]/CD45^{−}/7-AAD^{−} events. All samples were acquired on an LSRFortessa with HTS (BD Biosciences, San Jose, CA) and analyzed with FlowJo software (Tree Star, Ashland, OR).

Twenty-four–hour flow cytometric killing assay

Tumor cells (2×10^4) were plated in triplicate with the indicated ratios of NK cells in a 96-well plate. All wells contained 500 IU/ml rhIL-2 with 50% human NK cell medium and 50% tumor cell–specific medium. After coculture for 16–20 h at indicated E:T ratios, plates were washed and stained for flow cytometry, including Aldefluor expression (StemCell Technologies), for 30 min at 37°C per manufacturer's instructions. Tumor expression of CSC markers was established based on analysis of SSC^{hi}/CD45^{−}/7-AAD^{−} populations to exclude NK cells and nonviable cells. A discrete diethylaminobenzaldehyde control well was used for each E:T ratio to control for autofluorescence as well as ALDH signal degradation over time. To further standardize the ALDH signal, ALDH was gated as five times the median fluorescence intensity of the diethylaminobenzaldehyde sample.

Chromium-release assay

U87MG tumor cells were sorted into ALDH^{bright} and ALDH^{dim} populations. They were then allowed to recover for 48 h before labeling with 100 μCi sodium chromate (^{51}Cr; PerkinElmer, Boston, MA) for 1 h. Labeled cells (2×10^4) were incubated with activated NK cells at the indicated E:T ratios in 96-well plates for 4–7 h. Cytotoxicity was determined as described previously using a 1450 MicroBeta TriLux scintillation counter (PerkinElmer) (25).

In vitro mechanistic assays

NKG2D, NKp30, NKp44, and NKp46 Fc chimeras were purchased from R&D Systems (Minneapolis, MN) and added to cytotoxicity assays at 10 μg/ml along with 10 μg/ml donkey anti-human F(ab′)$_2$ fragments (Jackson ImmunoResearch Laboratories, West Grove, PA) to block Ab-dependent cellular cytotoxicity. Expression of NKG2D and NCR ligands was accomplished by staining tumor cells with 1 μg of the aforementioned Fc chimeras and detecting with a PE-conjugated anti-human secondary Ab (Jackson ImmunoResearch Laboratories).

In vivo tumor models

All in vivo experiments were performed with 8- to 20-wk-old female NOD Cg-*Prkdc^{scid} Il2rg^{tm1Wjl}*/SzJ (NSG) mice purchased from The Jackson Laboratory (Bar Harbor, ME). All experimental protocols were approved by the University of California Davis Institutional Animal Care and Use Committee. We used s.c., metastatic, and intrapancreatic tumor models. For s.c. models, mice received 10^6 tumor cells in 100 μl PBS in the rear flank. For metastatic tumor models, mice received 2.5×10^5 cells i.v. via tail vein. For intrapancreatic models, an upper laparotomy was perfomed, and 10^6 PANC-1 cells suspended in a 1:1 PBS/ Matrigel solution were orthotopically implanted into the pancreas of anesthetized mice. Tumor burden was assessed every 3–4 d by injecting 3 mg D-luciferin into anesthetized mice and recording bioluminescence with an IVIS Spectrum imaging station (Caliper Life Sciences, Hopkinton, MA).

Hydrodynamic IL-15 plasmid delivery

To maintain infused NK cells in an activated state in vivo, we injected an rhIL-15– producing plasmid as described previously (26). Plasmid (10 μg) was injected into mice via hydrodynamic delivery of 1.6 ml PBS i.v. in 4–6 s. Hydrodynamic IL-15 was administered 24 h before NK cell injection.

Immunofluorescence

Tissue samples for immunofluorescence were fixed overnight in 4% paraformaldehyde and then cryoprotected in 30% sucrose. Tissues were frozen in OCT and cut into 10-μm sections. Xenografted NK cells were detected with mouse anti-human CD56 (Abcam, Cambridge, MA). CD24-expressing PANC-1 cells were detected with rabbit anti-human Abs (Abcam). Abs conjugated to Alexa Fluor 488 or Alexa Fluor 594 (Jackson ImmunoResearch Laboratories) were used for secondary detection.

Statistical analysis

Categorical variables were compared using a χ^2 test. Parametric continuous variables were compared using an independent samples t test. Nonparametric continuous variables were compared using the Mann–Whitney U test. For comparison of more than two groups, statistical significance was determined using a one-way ANOVA followed by a Bonferroni multiple-group comparison test. Statistical analyses were performed using SAS version 9.2 (SAS Institute, Cary, NC) and GraphPad Prism 6. Significance was set at $p < 0.05$.

Results

Activated NK cells preferentially target CSCs in breast, glioma, sarcoma, and pancreatic tumor cell lines

Because cell lines represent a critical first step in understanding the biological processes of cancer, we first sought to test our hypothesis regarding the ability of NK cells to target CSC populations in these models. We focused on ALDH activity as a marker of CSCs because it provides a stable marker system that has been reported across a broad array of tumor cell types and because we have validated the CSC phenotype of ALDH^{bright} cells in our preclinical models (17). We also evaluated the cell surface markers CD24, CD44, and CD133 because these markers have been shown to identify CSC populations in breast cancer (CD24^{−}/CD44^{+}), pancreatic cancer (CD24^{+}/CD44^{+}), and glioblastoma (CD133).

As depicted in Fig. 1A, we observed populations of ALDH^{bright} cells for MDA-MB-231 (breast adenocarcinoma), U87MG (glioblastoma), A673 (Ewing's sarcoma), BxPC3 (pancreatic adenocarcinoma), and PANC-1 (pancreatic adenocarcinoma). We validated the stem-like phenotype of ALDH^{bright} U87MG cells by sorting purified populations of ALDH[bright] and ALDH^{dim} cells and injecting the sorted cells into the flanks of immunocompromised NSG mice (Supplemental Fig. 1A). Similarly, sorted cells from either population were plated into liquid culture and assessed for cell growth by MTT on the indicated days. We also injected 2×10^5 ALDH[bright] or unsorted A673 Ewing's sarcoma cells i.v. into NSG mice and observed these mice for tumor progression (Supplemental Fig. 1C). Harvested lungs and livers of mice that received sorted CSC-like cells showed a significantly higher tumor burden. These studies suggest that sorted ALDH^{bright} cells also show stem-like characteristics in sarcoma models via tumor formation.

We then coincubated allogeneic activated human NK cells with the indicated tumor cell lines for 18 h. With increasing E:T ratios, we observed significant reductions in the frequency of remaining live tumor cells that were ALDH[bright] (Fig. 1B). Furthermore, although both ALDH[bright] and ALDH[dim] populations were sensitive to NK cell cytotoxicity as assessed by total numbers of remaining live tumor cells (Fig. 1C), ALDH[bright] populations were significantly more susceptible to NK killing, resulting in greater reductions of the CSC population at lower NK cell ratios.

We also observed similar reductions in CSC populations after NK cell coculture when using other established markers for CSCs. For example, populations of CD133^{+} cells in the glioblastoma cell line U118 (Fig. 1D) and CD24^{+}/CD44^{+} cells in PANC-1 showed similar reductions in CSC populations after coculture with activated NK cells (Fig. 1E). In addition

to cytotoxicity assays with heterogeneous mixtures of stem/non–stem cells, purified populations of ALDH^{bright} cells were isolated by FACS and observed to have enhanced susceptibility to NK cell killing in a 4-h ^{51}Cr-release assay (Fig. 1F). These results indicate that NK cells can preferentially target the CSC populations of various tumor cell lines in vitro.

Fresh primary tumor specimens show enhanced susceptibility to allogeneic NK cells ex vivo

We then sought to determine whether NK cells were also capable of targeting CSCs from primary human cancer specimens. As shown in Fig. 2A, tumor tissue was obtained from patients with a diagnosis of well-differentiated liposarcoma (FSA1), Ewing's sarcoma (FSA2), and pancreatic ductal adenocarcinoma (FPA1 and FPA2). Primary tumor specimens were then dissociated into single-cell suspensions and incubated with increasing ratios of activated, allogeneic NK cells for 18 h before analysis by flow cytometry. Following exposure to NK cells, we observed a decrease in the proportion of CSCs within all of these primary tumor specimens (Fig. 2B). We observed a decrease in the frequency of CSCs after incubation with NK cells in soft-tissue sarcoma samples, similar to our observations with cell lines in Fig. 1. FPA1 was negative for both CD24 and CD44, but it showed decreased expression for ALDH when incubated with NK cells. FPA2 showed a decrease in CD24/CD44 as well as ALDH (CD24/CD44 depicted in Fig. 2B; the frequency and number of triple-positive CD24^{+}/CD44^{+}/ALDH^{bright} events shown in Fig. 2C and 2D, respectively). Total numbers of events showed a similar to trend to our data in cell lines. Although both populations of tumor cells were sensitive to cytotoxicity from activated NK cells, CSCs were most efficiently targeted (Fig. 2D). For additional validation, purified CSCs (CD24^{+}/CD44^{+}/ALDH^{bright}) or non-CSCs (CD24^{−}/ALDH^{dim}) from FPA2 were sorted by FACS and incubated with activated NK cells in an 18-h cytotoxicity assay (Fig. 2E). In this assay, purified populations of CSCs were highly sensitive to NK cells, similar to our results in the above experiments using heterogeneous populations of tumor cells.

Autologous NK cells can effectively kill primary CSCs

Given increasing evidence that NK cells become maximally activated and cytotoxic when they recognize "missing-self" Ags, we obtained matched peripheral blood from patients undergoing tumor resection to assess the ability of autologous NK cells to target CSCs. In this study, after 24 h activation in rhIL-2, we incubated NK cells with dissociated tumor cells for 16 h. Standard blood samples from healthy donors were used as an allogeneic control.

As shown in Fig 3A–C, autologous NK cells demonstrated equivalent cytotoxicity against CSC populations from two primary leiomyosarcomas (FSA3 and FSA4) based on reductions in ALDH[bright] populations. These data suggest that autologous NK cells are equally as capable as allogeneic NK cells at targeting CSCs in primary solid tumors when expanded and activated with cytokine-based stimulation techniques. Additionally, we compared NK killing from patients and healthy donors against HLA[−] K562 targets (data not shown) and observed equivalent tumor cell killing, further supporting the concept that autologous NK cells were not overtly dysfunctional after activation with rh-IL2.

To test the impact of prior IL-2 activation on NK cell cytotoxicity toward CSCs, NK cells were collected from a patient undergoing resection of a leiomyosarcoma (FSA5) 7 d prior and on the day of the cancer resection. NK cells collected 7 d prior to the resection were activated and expanded ex vivo as before, whereas those cells collected on the same day as the tumor resection were not stimulated. The sarcoma was processed into single-cell suspension per standard protocol and cocultured with increasing doses of both groups of NK cells. We performed flow cytometry for CSC identification by ALDH expression and observed no change in CSC frequency with resting NK cells (Fig. 3D). This indicates that cytokine activation is necessary to achieve maximal lysis of CSCs by NK cells.

Stress-related surface protein expression on CSCs

We next investigated the role of NK cell activation receptor ligands and death receptors as a potential mechanism for CSC recognition and killing. As shown in Fig. 4A and 4B, flow cytometric staining of a primary pancreatic adenocarcinoma (FPA2) demonstrated greater surface expression of NKG2D ligands (MICA/B) and the death receptors Fas and DR5 on CSCs versus non-CSCs. Surface expression of NCR ligands via receptor/Fc fragment chimeras did not reveal expression of NCR ligands on the primary tumors probed (data not shown). We observed a similar pattern of overexpression of these stress-related proteins on CSCs in a primary Ewing's sarcoma (Fig. 4C). Analysis by quantitative RT-PCR demonstrated transcriptional upregulation of NKG2D ligands and death receptors on the sorted CSC population compared with non-CSCs in both a primary pancreatic carcinoma (Fig. 4D) and a Ewing's sarcoma (Fig. 4E). These sorted primary tumor samples showed levels of CSC-related transcripts consistent with their flow cytometric phenotypes. Alternatively, we detected no difference in HLA expression between CSC and non-CSC populations in these primary cancers as measured by a pan–HLA-ABC Ab, although HLA-ABC expression was very low and near the limit of detection by flow cytometry in these samples (data not shown). Collectively, our data implicate upregulation of NKG2D ligands and death receptors in the mechanism of NK targeting of CSCs.

Blocking NK cell activation ligands reverses NK cell killing of CSCs

To assess the functional consequences of NK recognition ligand expression on CSCs, we performed in vitro blocking studies utilizing Fc chimeric proteins. As shown in Fig. 5A and 5C, blockade of NKG2D significantly inhibited NK killing of whole tumor populations in the primary pancreatic adenocarcinoma sample (FPA2) and PANC-1 cell line. In contrast, blockade of other NK-activating ligands did not reverse NK killing compared with isotype control. We observed similar effects on NKG2D-mediated NK killing of CSCs as assessed by overall cell numbers and percentage of CSCs after NK coculture (Fig. 5B, 5D). Taken together, these data show that blockade of NKG2D ligands diminished the overall killing of unsorted target cells (Fig. 5A, C), although it is notable that, by itself, NKG2D blockade was insufficient to completely abrogate NK cell specificity toward CSCs in the primary pancreatic cancer (Fig. 5B).

Additionally, we did not observe differences in NK cytotoxicity toward CSCs when blocking NCR ligands NKp30, NKp44, and NKp46 in either cell lines or primary cancers, further supporting our hypothesis that NK targeting of CSCs occurs via an NKG2D-

dependent mechanism. To further determine the molecular mechanism of the NK-mediated decrease in CSCs, we blocked granule-mediated cytotoxicity of NK cells with concanamycin A (CMA) or inhibited apoptosis on PANC-1 targets via the pan-caspase inhibitor Z-VAD. In a 24-h cytotoxicity assay (Fig. 5E), at high NK to tumor ratios (5:1), we observed a complete eradication of ALDH-expressing CSCs. However, we observed a diminished capacity of NK cells to target CSCs when blocking granule-mediated killing by CMA or apoptotic pathways with Z-VAD. These data implicate both granule-mediated and death ligand pathways in preferential NK killing of CSCs and corroborate our previous data showing higher levels of NKG2D ligands and death receptors on CSCs compared with the non-CSC populations.

NK cells target CSCs in vivo

We next assessed whether adoptive transfer of NK cells would target human CSCs in vivo. Subcutaneous xenografts were established from multiple cell lines and allowed to establish tumors. We then injected ex vivo–activated NK cells into tumors and assessed CSC populations. As shown in Fig. 6A and 6B, we observed marked decreases in CSCs following NK treatment when enumerated by either ALDH expression (A673, U87, and PANC-1 xenografts) or CD24 (PANC-1; Fig. 6B). Analysis of xenograft tumor specimens by flow cytometry up to 10 d following NK transfer revealed that engrafted NK cells persisted in the tumor (data not shown), and immunofluorescence revealed that NK cells colocalized to tumor areas enriched for CSCs (Fig. 6C), further suggesting that NK cells can seek out CSCs in vivo following adoptive transfer.

Ex vivo–activated NK cells were next used as a treatment in a metastatic model of breast carcinoma (MDA-MB-231) in which tumor cells were administered i.v. and mice developed tumors predominantly in the lungs and liver. Twenty-five days after tumor infusion, we injected 20×10^6 NK cells i.v., and 5 d later, mice were sacrificed. In this brief treatment period, we also observed a reduced number of tumor colonies when homogenized lung cells were plated in lung colony formation assays (Fig. 6D). Interestingly, colonies that did develop in NK cell–treated mice showed an impressive reduction in size (Fig. 6E), consistent with NK cell targeting of stem-like tumor cells.

Given the reduction in CSC numbers in our s.c. and metastatic in vivo models, we next assessed the therapeutic effects of NK cells in an orthotopic pancreatic cancer model. Mice with established orthotopic PANC-1 tumors were treated with i.v. NK cells and assessed for tumor burden by bioluminescence imaging. Twenty days after NK treatment, mice treated with NK cell transfer showed a trend toward decreased bioluminescence when compared with untreated mice (Fig. 6F, 6G). Taken together, these results show that NK cells can effectively target CSCs in vivo, and this targeting by NK cells appears capable of delaying tumor progression.

Discussion

Molecular and genetic tumor heterogeneity is widely recognized, but a growing body of literature supports the hypothesis that cancers are comprised of a heterogeneous population of malignant cells. Moreover, there is convincing evidence that tumors are composed of a

hierarchical structure spanning the spectrum from terminally differentiated cells to rapidly amplifying cells to cells with stem cell–like properties that are capable of reconstituting the entire bulk tumor, including all of its cell types (2, 4, 27). It is these CSCs that are also able to resist antiproliferative therapies and seed metastasis.

Given the evidence that CSCs are clinically and biologically relevant as both drivers of resistance to standard cytotoxic therapies and markers of worse oncologic outcome, therapeutic targeting of CSCs has emerged as an unmet need in clinical and translational oncology. In this study, utilizing extensive ex vivo and in vivo models to demonstrate preferential NK killing of CD24^{+}/CD44^{+}, CD133^{+}, and ALDH^{bright} CSCs compared with the corresponding non-CSC populations, we demonstrate that activated NK cells act as efficient immune effector cells targeting CSCs. Additionally, our data indicate that these NK–CSC interactions occur in an NKG2D-dependent manner, suggesting an important area for future research to both optimize the therapeutic benefits as well as to design methods to prevent potential immune evasion. Although we rely on cell surface markers and the intracellular enzyme ALDH to identify CSC subpopulations in our models, we also provide important functional data validating the CSC phenotype of CSCs identified by cells surface markers and ALDH. Additionally, we and others have carefully validated these CSC markers in diverse solid tumors, including breast cancer, pancreatic cancer, and sarcoma. Overall, the emerging data support the concept that CSCs are important to cancer biology. Therefore, it will be important to design strategies to target CSC subsets within tumors to prevent relapse.

In the past decade, there have been significant advances in the field of CSC biology. The emerging evidence has demonstrated that CSCs play critical roles in drug resistance, invasion, and metastasis. Furthermore, although CSCs and non-CSCs within the same tumor share similar genetic fingerprints, there are distinct transcriptional patterns observed between CSCs and non-CSCs, highlighting the importance of plasticity and epigenetic phenomena in regulating CSCs and non-CSCs. For example, the activation of disparate pathways, such as hedgehog, TGF-β, and Wnt/β-catenin, between CSCs and non-CSCs suggests that effective therapy may require selective targeting of these distinct cell populations.

Our results suggest that NK cells possess an innate ability to recognize and kill solid tumor CSCs. There are several key advantages to harnessing NK cells (19). First, NK cells are Ag nonspecific and therefore do not require the expression of a specific Ag on a given HLA allotype. CSCs have recently been demonstrated to be highly susceptible to NK cell attack, suggesting that NK cells may be useful as part of a combined modality approach capable of targeting CSC and non-CSC populations. Tseng et al. (28), for example, demonstrated in both human and mouse models that stage of differentiation for both malignant and embryonic cells predicted their sensitivity to NK cell lysis. These authors also reported that inhibition of differentiation or reversion of cells to a less differentiated phenotype by blocking NF-κB or targeted knockdown of COX2 significantly increased NK cell effector functions. Tallerico et al. (29) demonstrated that freshly purified allogeneic NK cells can recognize and kill colorectal cancer-initiating cells (CICs) whereas the non-CIC counterpart of the tumors was less susceptible to NK cells. In contrast to our findings, Tallerico et al.

observed that the difference in the NK cell susceptibility was correlated with higher expression on CICs of ligands for NKp30 and NKp44 in the natural cytotoxicity receptor group of activating NK receptors. Additionally, CICs were shown to express lower levels of MHC class I on their surface than the "differentiated" tumor cells, and MHC class I molecules are known to inhibit NK recognition and function.

Although these studies were consistent with our findings that NK cells have the capacity to kill CSCs (29, 30), note that the authors' results appeared to be highly dependent on serum starvation in their cell culture conditions. Although serum deprivation is an important technique to promote the growth and phenotype of stem-like tumor cells, it also promotes sensitivity to apoptosis-inducing pathways (31, 32) and may artificially enhance NK sensitivity to these targets. Therefore, an important strength of our study is our extensive use of unmanipulated primary solid tumors to examine CSC and non-CSC populations in ex vivo models. Moreover, our use of these models may more closely recapitulate the interaction of NK cells with various tumor populations in vivo.

The enhanced sensitivity of CSCs to NK cells seems counterintuitive at first given that CSCs have been described as quiescent (33), and high rates of proliferation have previously been shown to correlate with sensitivity to NK cells (34). However, recent data have shown that less differentiated cells, including embryonic stem cells, induced pluripotent stem cells, and mesenchymal stem cells, are more sensitive to NK cell killing than their differentiated progeny (35). The phenotype of these cell types is associated with lower or undetectable levels of MHC class I molecules, and it is plausible to hypothesize that NK cells may thus have an important regulatory function in suppressing the growth of stem-like cell types. This hypothesis is also supported by a well-established body of literature showing a lack of graft-versus-host reactions when allogeneic NK cells are exposed to mature, solid tissues after hematopoietic stem cell transplantation, despite NK recognition of host hematopoietic stem cells (36). Phenotypic similarities between normal stem cells and CSCs may thereby explain the higher sensitivity of these cells to NK killing. Our data suggest that immunotherapy using NK cells can be used as part of a combination strategy to eliminate CSCs from a wide array of solid tumors.

A potential limitation of our study is the limited data demonstrating in vivo efficacy of this approach, especially using immunocompetent preclinical models. For examples, key studies have observed mechanisms of CSC evasion of immunosurveillance through shedding of MICA and MICB as well as apparent CSC recruitment of regulatory T cells to promote an immune-privileged state. The results of these studies highlight a fundamental point of the immune system with respect to CSCs or any other target cell, namely that it can be primed both for and against immune targeting. It will be important to recognize and address these potential limitations to ensure that optimal results from this novel immunotherapy approach are realized.

In summary, activated NK cells appear to preferentially target cancer cells with a CSC phenotype. These data emphasize the potential clinical application of NK immunotherapy given the increasing evidence in the literature that CSCs are a mechanism of resistance and relapse in solid malignancies following conventional cytotoxic therapies. There is significant

optimism that a multimodality approach using immunotherapy in combination with cytotoxic treatments to simultaneously eradicate CSCs and non-CSCs will lead to more complete and durable cancer eradication. Our results suggest that NK targeting of CSCs holds significant promise in the ultimate goal of overcoming cancer resistance and curing more patients with cancer.

Supplementary Material

Refer to Web version on PubMed Central for supplementary material.

Acknowledgments

Abbreviations used in this article

7-AAD	7-aminoactinomycin D
ALDH	aldehyde dehydrogenase
CIC	cancer-initiating cell
CMA	concanamycin A
CSC	cancer stem cell
NSG	NOD.Cg-*Prkdc^{scid} Il2rg^{tm1Wjl}*/SzJ
rh	recombinant human
SSC	side scatter

References

1. Visvader JE, Lindeman GJ. Cancer stem cells: current status and evolving complexities. Cell Stem Cell. 2012; 10:717–728. [PubMed: 22704512]

2. Chen J, Li Y, Yu TS, McKay RM, Burns DK, Kernie SG, Parada LF. A restricted cell population propagates glioblastoma growth after chemotherapy. Nature. 2012; 488:522–526. [PubMed: 22854781]

3. Valent P, Bonnet D, De Maria R, Lapidot T, Copland M, Melo JV, Chomienne C, Ishikawa F, Schuringa JJ, Stassi G, et al. Cancer stem cell definitions and terminology: the devil is in the details. Nat Rev Cancer. 2012; 12:767–775. [PubMed: 23051844]

4. Driessens G, Beck B, Caauwe A, Simons BD, Blanpain C. Defining the mode of tumour growth by clonal analysis. Nature. 2012; 488:527–530. [PubMed: 22854777]

5. Wang L, Park P, Zhang H, La Marca F, Lin CY. Prospective identification of tumorigenic osteosarcoma cancer stem cells in OS99-1 cells based on high aldehyde dehydrogenase activity. Int J Cancer. 2011; 128:294–303. [PubMed: 20309879]

6. Charafe-Jauffret E, Ginestier C, Bertucci F, Cabaud O, Wicinski J, Finetti P, Josselin E, Adelaide J, Nguyen TT, Monville F, et al. ALDH1-positive cancer stem cells predict engraftment of primary

breast tumors and are governed by a common stem cell program. Cancer Res. 2013; 73:7290–7300. [PubMed: 24142344]

7. Charafe-Jauffret E, Ginestier C, Iovino F, Tarpin C, Diebel M, Esterni B, Houvenaeghel G, Extra JM, Bertucci F, Jacquemier J, et al. Aldehyde dehydrogenase 1-positive cancer stem cells mediate metastasis and poor clinical outcome in inflammatory breast cancer. Clin Cancer Res. 2010; 16:45–55. [PubMed: 20028757]

8. Deng S, Yang X, Lassus H, Liang S, Kaur S, Ye Q, Li C, Wang LP, Roby KF, Orsulic S, et al. Distinct expression levels and patterns of stem cell marker, aldehyde dehydrogenase isoform 1 (ALDH1), in human epithelial cancers. PLoS One. 2010; 5:e10277. [PubMed: 20422001]

9. Douville J, Beaulieu R, Balicki D. ALDH1 as a functional marker of cancer stem and progenitor cells. Stem Cells Dev. 2009; 18:17–25. [PubMed: 18573038]

10. Ginestier C, Hur MH, Charafe-Jauffret E, Monville F, Dutcher J, Brown M, Jacquemier J, Viens P, Kleer CG, Liu S, et al. ALDH1 is a marker of normal and malignant human mammary stem cells and a predictor of poor clinical outcome. Cell Stem Cell. 2007; 1:555–567. [PubMed: 18371393]

11. Hermann PC, Huber SL, Herrler T, Aicher A, Ellwart JW, Guba M, Bruns CJ, Heeschen C. Distinct populations of cancer stem cells determine tumor growth and metastatic activity in human pancreatic cancer. Cell Stem Cell. 2007; 1:313–323. [PubMed: 18371365]

12. Rasheed Z, Wang Q, Matsui W. Isolation of stem cells from human pancreatic cancer xenografts. J Vis Exp. 2010; (43):2169. [PubMed: 20972397]

13. Rasheed ZA, Yang J, Wang Q, Kowalski J, Freed I, Murter C, Hong SM, Koorstra JB, Rajeshkumar NV, He X, et al. Prognostic significance of tumorigenic cells with mesenchymal features in pancreatic adenocarcinoma. J Natl Cancer Inst. 2010; 102:340–351. [PubMed: 20164446]

14. Awad O, Yustein JT, Shah P, Gul N, Katuri V, O'Neill A, Kong Y, Brown ML, Toretsky JA, Loeb DM. High ALDH activity identifies chemotherapy-resistant Ewing's sarcoma stem cells that retain sensitivity to EWS-FLI1 inhibition. PLoS One. 2010; 5:e13943. [PubMed: 21085683]

15. Jiang X, Gwye Y, Russell D, Cao C, Douglas D, Hung L, Kovar H, Triche TJ, Lawlor ER. CD133 expression in chemo-resistant Ewing sarcoma cells. BMC Cancer. 2010; 10:116. [PubMed: 20346143]

16. Lohberger B, Rinner B, Stuendl N, Absenger M, Liegl-Atzwanger B, Walzer SM, Windhager R, Leithner A. Aldehyde dehydrogenase 1, a potential marker for cancer stem cells in human sarcoma. PLoS One. 2012; 7:e43664. [PubMed: 22928012]

17. Canter RJ, Ames E, Mac S, Grossenbacher SK, Chen M, Li CS, Borys D, Smith RC, Tellez J, Sayers TJ, et al. Anti-proliferative but not anti-angiogenic tyrosine kinase inhibitors enrich for cancer stem cells in soft tissue sarcoma. BMC Cancer. 2014; 14:756. [PubMed: 25301268]

18. Penchev VR, Rasheed ZA, Maitra A, Matsui W. Heterogeneity and targeting of pancreatic cancer stem cells. Clin Cancer Res. 2012; 18:4277–4284. [PubMed: 22896694]

19. Ames E, Murphy WJ. Advantages and clinical applications of natural killer cells in cancer immunotherapy. Cancer Immunol Immunother. 2014; 63:21–28. [PubMed: 23989217]

20. Klingemann HG. Cellular therapy of cancer with natural killer cells-where do we stand? Cytotherapy. 2013; 15:1185–1194. [PubMed: 23768925]

21. Barao I, Murphy WJ. The immunobiology of natural killer cells and bone marrow allograft rejection. Biol Blood Marrow Transplant. 2003; 9:727–741. [PubMed: 14677112]

22. Liao T, Kaufmann AM, Qian X, Sangvatanakul V, Chen C, Kube T, Zhang G, Albers AE. Susceptibility to cytotoxic T cell lysis of cancer stem cells derived from cervical and head and neck tumor cell lines. J Cancer Res Clin Oncol. 2013; 139:159–170. [PubMed: 23001491]

23. Di Tomaso T, Mazzoleni S, Wang E, Sovena G, Clavenna D, Franzin A, Mortini P, Ferrone S, Doglioni C, Marincola FM, et al. Immunobiological characterization of cancer stem cells isolated from glioblastoma patients. Clin Cancer Res. 2010; 16:800–813. [PubMed: 20103663]

24. Berg M, Lundqvist A, McCoy P Jr, Samsel L, Fan Y, Tawab A, Childs R. Clinical-grade ex vivo-expanded human natural killer cells up-regulate activating receptors and death receptor ligands and have enhanced cytolytic activity against tumor cells. Cytotherapy. 2009; 11:341–355. [PubMed: 19308771]

25. Ames E, Hallett WH, Murphy WJ. Sensitization of human breast cancer cells to natural killer cell-mediated cytotoxicity by proteasome inhibition. Clin Exp Immunol. 2009; 155:504–513. [PubMed: 19220837]

26. Barao I, Alvarez M, Redelman D, Weiss JM, Ortaldo JR, Wiltrout RH, Murphy WJ. Hydrodynamic delivery of human IL-15 cDNA increases murine natural killer cell recovery after syngeneic bone marrow transplantation. Biol Blood Marrow Transplant. 2011; 17:1754–1764. [PubMed: 21906575]

27. Schepers AG, Snippert HJ, Stange DE, van den Born M, van Es JH, van de Wetering M, Clevers H. Lineage tracing reveals Lgr5$^+$ stem cell activity in mouse intestinal adenomas. Science. 2012; 337:730–735. [PubMed: 22855427]

28. Tseng HC, Arasteh A, Paranjpe A, Teruel A, Yang W, Behel A, Alva JA, Walter G, Head C, Ishikawa TO, et al. Increased lysis of stem cells but not their differentiated cells by natural killer cells; de-differentiation or reprogramming activates NK cells. PLoS One. 2010; 5:e11590. [PubMed: 20661281]

29. Tallerico R, Todaro M, Di Franco S, Maccalli C, Garofalo C, Sottile R, Palmieri C, Tirinato L, Pangigadde PN, La Rocca R, et al. Human NK cells selective targeting of colon cancer-initiating cells: a role for natural cytotoxicity receptors and MHC class I molecules. J Immunol. 2013; 190:2381–2390. [PubMed: 23345327]

30. Avril T, Vauleon E, Hamlat A, Saikali S, Etcheverry A, Delmas C, Diabira S, Mosser J, Quillien V. Human glioblastoma stem-like cells are more sensitive to allogeneic NK and T cell-mediated killing compared with serum-cultured glioblastoma cells. Brain Pathol. 2012; 22:159–174. [PubMed: 21790828]

31. Takashina T, Nakayama M. Modifications enhance the apoptosis-inducing activity of FADD. Mol Cancer Ther. 2007; 6:1793–1803. [PubMed: 17575108]

32. Holmström TH, Tran SE, Johnson VL, Ahn NG, Chow SC, Eriksson JE. Inhibition of mitogen-activated kinase signaling sensitizes HeLa cells to Fas receptor-mediated apoptosis. Mol Cell Biol. 1999; 19:5991–6002. [PubMed: 10454546]

33. Gao MQ, Choi YP, Kang S, Youn JH, Cho NH. CD24$^+$ cells from hierarchically organized ovarian cancer are enriched in cancer stem cells. Oncogene. 2010; 29:2672–2680. [PubMed: 20190812]

34. Mistry AR, O'Callaghan CA. Regulation of ligands for the activating receptor NKG2D. Immunology. 2007; 121:439–447. [PubMed: 17614877]

35. Jewett A, Man YG, Tseng HC. Dual functions of natural killer cells in selection and differentiation of stem cells; role in regulation of inflammation and regeneration of tissues. J Cancer. 2013; 4:12–24. [PubMed: 23386901]

36. Asai O, Longo DL, Tian ZG, Hornung RL, Taub DD, Ruscetti FW, Murphy WJ. Suppression of graft-versus-host disease and amplification of graft-versus-tumor effects by activated natural killer cells after allogeneic bone marrow transplantation. J Clin Invest. 1998; 101:1835–1842. [PubMed: 9576746]
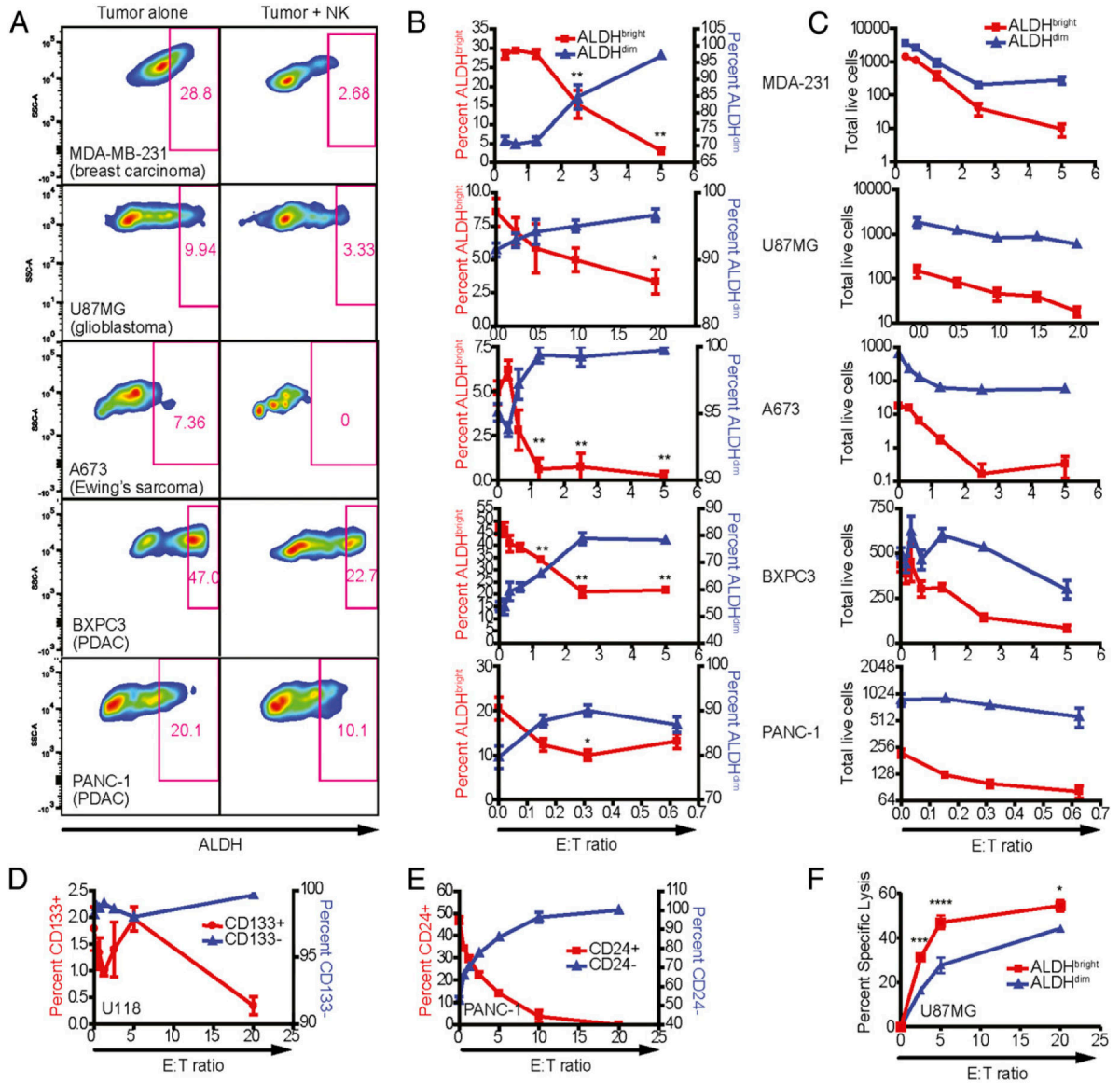
FIGURE 1.

Sensitivity of human tumor cell lines to NK cell lysis. Human NK cells were activated with IL-2, expanded for 2 wk, and cocultured 16–18 h with MDA-MB-231 (breast adenocarcinoma), U87MG (glioblastoma), A673 (Ewing's sarcoma), BxPC3 (pancreatic ductal adenocarcinoma), and PANC-1 (pancreatic ductal adenocarcinoma) in the presence of 500 IU/ml rhIL-2. Phenotypes of remaining tumor cells were assessed by excluding 7-AAD[+] events. (**A**) ALDH expression was assessed using the Aldefluor system in cultures with tumor cells alone and with NK cells at E:T ratios between 1:1 and 5:1. (**B**) The percentage of ALDH[bright] events on tumor cells was plotted (red; left *y*-axis) against the ALDH[dim] population (blue; right *y*-axis) at the indicated E:T ratios. (**C**) The total number of acquired events from (B) were plotted over the indicated E:T ratios. Reductions in ALDH[bright] populations in comparison with untreated cells were determined via one-way ANOVA with a Tukey posttest. *$p < 0.05$; **$p < 0.01$. (**D**) CSCs from the U118 glioblastoma were

identified based on expression of surface marker CD133 (glioblastoma) following culture with NK cells at the specified E:T ratios. (**E**) Changes in the proportions of CD24-expressing and nonexpressing PANC-1 cells following NK coculture. (**F**) U87-MG cells were sorted for ALDH expression and then assessed for sensitivity to NK cell cytotoxicity in a 4-h ^{51}Cr-release assay.
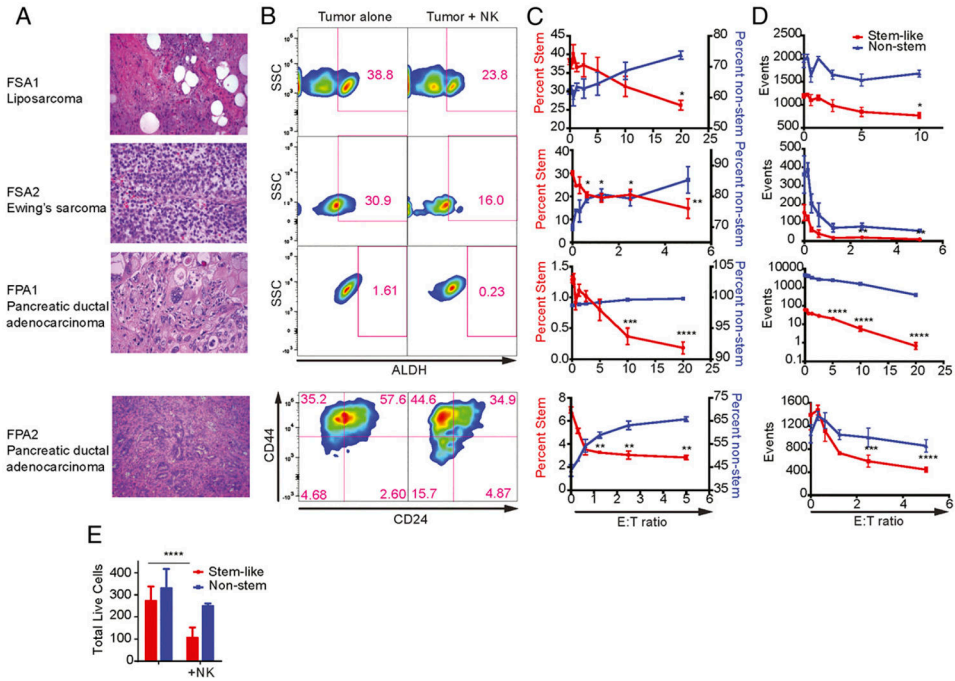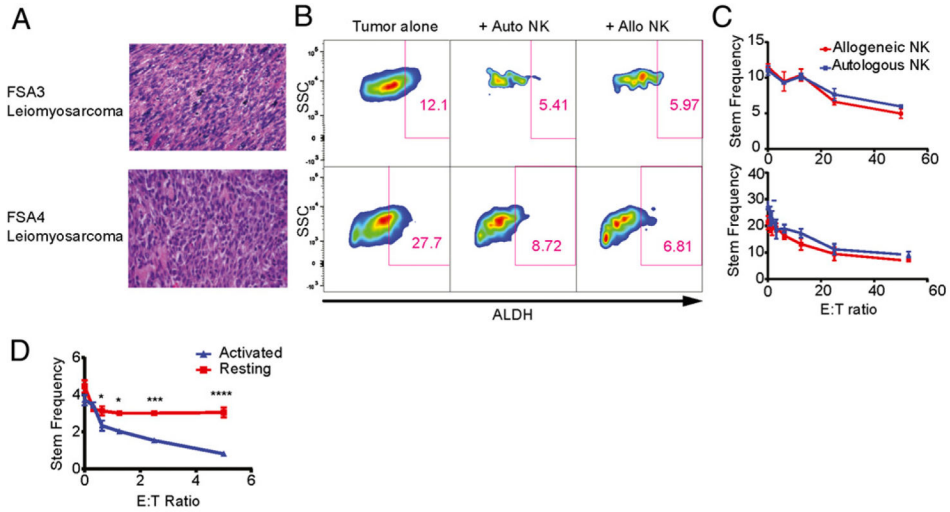
FIGURE 2.
CSCs from human primary tumors are preferentially targeted by human NK cells. (**A**) Well-differentiated liposarcoma (FSA1), Ewing's sarcoma (FSA2), and pancreatic ductal adenocarcinoma (FPA1 and FPA2) were obtained from fresh clinical specimens (H&E staining, original magnification ×40). (**B**) ALDH or CD24/CD44 expression on tumor targets was assessed with tumor cells alone or those cocultured with NK cells at E:T ratios between 1:1 and 5:1. (**C**) The percentage of CSC populations on tumor cells was plotted (red; left *y*-axis) against the non-CSC population (blue; right *y*-axis) at the indicated E:T ratios. (**D**) The total number of acquired events from (**B**) were plotted over the indicated E:T ratios. (**E**) Stem-like (CD24$^+$/CD44$^+$/ALDH^{bright}) or non–stem cells (CD24$^-$/ALDH^{dim}) from FPA2 were sorted then used in a 16-h NK cell cytotoxicity assay with allogeneic NK cells. Reductions in CSC populations were determined via one-way ANOVA with a Tukey posttest. *$p < 0.05$, ** $p < 0.01$, ***$p < 0.001$, ****$p < 0.0001$.

FIGURE 3.

Autologous NK cells can effectively kill primary CSCs. (**A**) Fresh primary leiomyosarcomas FSA3 and FSA4 were processed into single-cell suspensions and used in cytotoxicity assays with either patient-matched autologous or healthy donor allogeneic NK cells (H&E staining, original magnification ×40). (**B**) ALDH expression of tumor cells was assessed by excluding CD45^{+} and 7-AAD^{+} events. (**C**) The percentages of ALDH^{bright} tumor cells were determined following coculture with either autologous or allogeneic NK cells at E:T ratios ranging from 0 to 50. (**D**) NK cells were isolated from a patient both on the day of the resection of a leiomyosarcoma or 7 d before. NK cells isolated 7 d before the resection were activated with IL-2 as before whereas those isolated on the same day as the tumor were left unactivated. Both batches of NK cells were cultured with tumor cell suspensions in a flow cytometric cytotoxicity assay at the indicated E:T ratios. The percentage of remaining tumor cells showing a CSC-like phenotype via ALDH expression are shown and differences between resting and activated NK cells were determined via two-way ANOVA with a Sidak multiple comparisons test. $*p < 0.05$, $***p < 0.001$, $****p < 0.0001$.
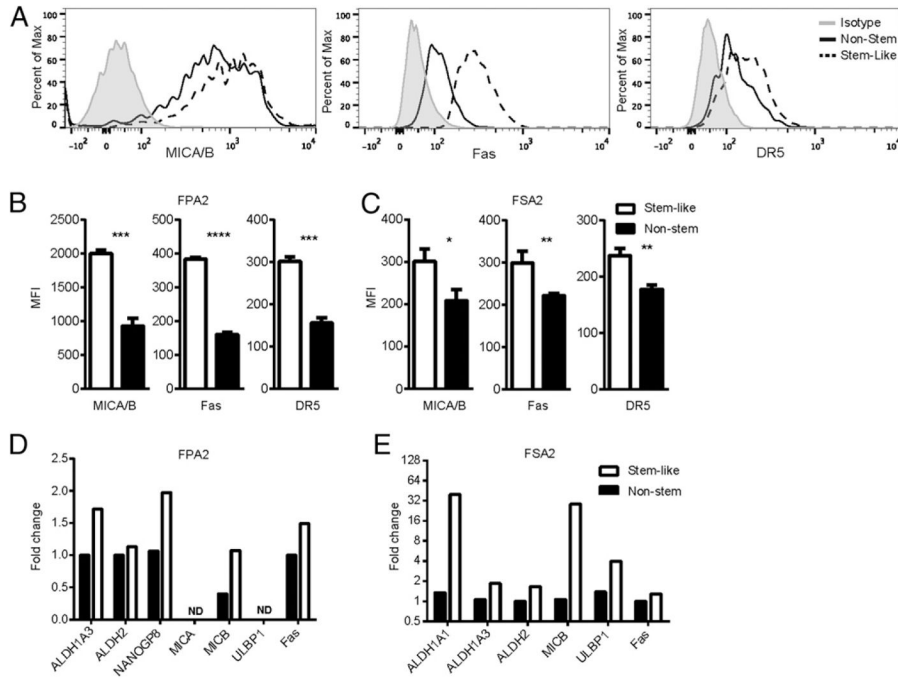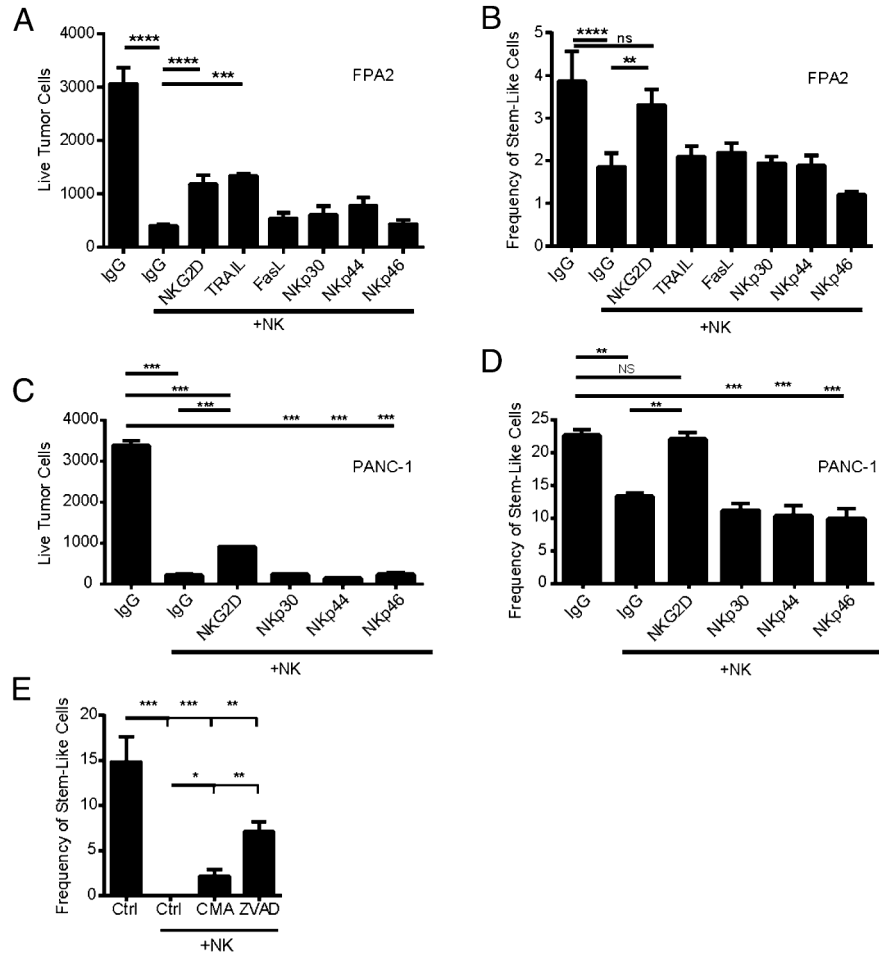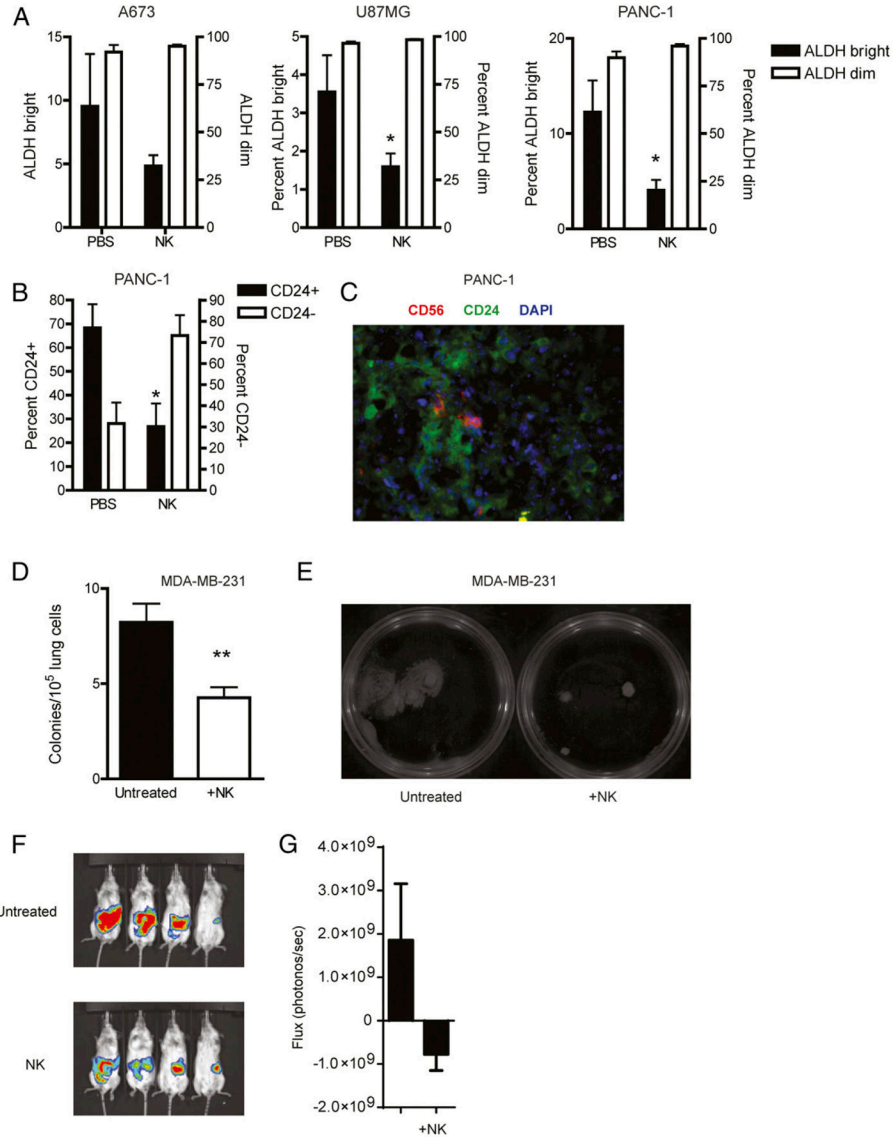
FIGURE 4.
CSCs express higher levels of NKG2D ligands and death receptors than do non-CSCs. (**A**) Histograms of median fluorescence intensity (MFI) of MICA/B, Fas, and DR5 by flow cytometry are shown from CSC (dotted lines) and non-CSC (solid lines) populations from the primary pancreatic adenocarcinoma, FPA2. Quantified MFI values are shown for FPA2 (**B**) and a soft-tissue sarcoma (FSA2) (**C**). CSC populations from these tumor specimens were sorted and assessed by quantitative RT-PCR for CSC markers and stress ligands on FPA2 (**D**) and FSA2 (**E**). *$p < 0.05$, **$p < 0.01$, ***$p < 0.001$.

FIGURE 5.

Blocking NKG2D abrogates NK killing of CSCs from cell lines and primary tumors. FPA2 (**A** and **B**) or PANC-1 (**C** and **D**) cells were cultured with activated NK cells (1:1 E:T ratio) for 16 h in the presence of the indicated Fc-chimeric proteins that blocked the indicated activation receptors. Human IgG1 purified Ab was added as an isotype-matched control. Tumors were then analyzed by flow cytometry for total numbers of remaining live tumor cells (SSC^{hi}CD45$^-$7-AAD$^-$) (A and C) and percentages of tumor cells expressing CD24/CD44/ALDH^{bright} (B and D). (**E**) PANC-1 cells were pretreated with 80 μM ZVAD or vehicle control for 1 h, or NK cells were pretreated with 50 nM CMA for 1 h. NK cells and PANC-1 tumor cells were then mixed at a 5:1 ratio and ZVAD, CMA, or vehicle controls were adjusted to maintain the above-stated concentrations. Twenty-four hours later, wells were harvested and analyzed for ALDH expression by flow cytometry. Reductions in stem-like populations in comparison with untreated cells were determined via one-way ANOVA with a Tukey posttest. $*p < 0.05$, $**p < 0.01$, $***p < 0.001$, $****p < 0.0001$.

FIGURE 6.

NK cells attack CSCs in vivo. Mice bearing s.c. A673, U87, and PANC-1 tumors were intratumorally injected with 2×10^7 activated NK cells. Six days later, mice were sacrificed and tumors were processed into single-cell suspensions and assessed for ALDH (**A**) or CD24 (**B**) expression. ALDH^{bright} or CD24 (CSC) percentages are plotted on the left *y*-axis and ALDH^{dim} or CD24$^-$ (non-CSC) percentages are plotted on the right *y*-axis. (**C**) Colocalization of transferred NK cells and CD24-expressing CSCs was detected using immunofluorescence (anti-CD56, red; anti-CD24, green; DAPI, blue; original magnification ×40). (**D**) Lungs from mice bearing metastatic MDA-MB-231 tumors were plated in CFU assays 5 d after in vivo NK cell injections. The number of tumor colonies were counted (**D**) and imaged for comparison (**E**). NSG mice were given orthotopic injections of PANC-1 into the pancreas. Twenty days following tumor implantation, 2×10^7 activated NK cells were injected i.v. Bioluminescent images (**F**) and combined values (**G**) were assessed 14 d after

NK cell transfer. Experiments were performed twice with three to four mice per group. Statistics were determined by one-way ANOVA with a Bonferroni posttest (A and B) or Student t test (C, D, and G). *$p < 0.05$, **$p < 0.01$.